Recognizing common PET patterns in neurodegenerative dementia

Yin Jie Chen, MD; Jacob G. Dubroff, MD, PhD; and Ilya M. Nasrallah, MD, PhD

Neurodegeneration, primarily due to Alzheimer's disease (AD), is the major cause of dementia.[1,2] Age is a major risk factor for AD and the prevalence of dementia is predicted to increase dramatically with the growing elderly population.[1] After AD, the most common neurodegenerative causes of dementia are dementia with Lewy bodies (DLB) and frontotemporal lobar degeneration (FTLD). Vascular dementia is the only non-neurodegenerative cause of dementia with a similar prevalence.[3] Classically, neurodegenerative diseases tend to most strongly affect specific cognitive domains related to the specific pattern of neurodegeneration – memory for AD, for example – but there can be syndromic overlap especially early in the course of the disease.

This article reviews the appearances of the common neurodegenerative dementia on positron emission tomography (PET), specifically ^{18}F-fluorodeoxyglucose (FDG) PET and amyloid PET, with the goal of increasing diagnostic accuracy and confidence of practicing radiologists in the use of PET for differentiating types of dementia.

Dr. Chen, Dr. Dubroff, and Dr. Nasrallah are Radiologists at the Hospital of the University of Pennsylvania, Philadelphia, PA.
Disclosure: Dr. Nasrallah receives research support from Avid Radiopharmaceuticals, a producer of one of the amyloid PET radioligands discussed in this article.

Neurodegenerative disease and the role of ^{18}F-FDG PET

The region of the brain affected varies with each neurodegenerative disease, but the underlying pathophysiology is the same: progressive neuronal dysfunction and loss, ultimately resulting in cognitive decline. Each cause has characteristic clinical symptoms and affects particular cognitive domains. Alzheimer's disease, for example, shows decline in memory. The similarities in clinical presentation among these diseases, moreover, frequently lead to diagnostic uncertainty, especially early on, when symptoms are milder and typical cognitive findings are only partially expressed. In fact, when patients begin to show the earliest objective signs of cognitive decline, the term Mild Cognitive Impairment (MCI) is often used until a more certain diagnosis can be achieved.

During the past several decades – the last 15 years, in particular – advances in imaging have provided biomarkers to assist in diagnosis and provide prognostic information in neurodegenerative dementia. ^{18}F-FDG uptake by the brain is one such biomarker of integrated metabolic activity, reflecting a combination of blood flow, gray matter volume, and synaptic function,[4] all of which are affected by neurodegeneration. As such, ^{18}F-FDG as a biomarker is not specific to a particular cause of dementia, but rather an identifier of regional neurodegeneration.

Although there is some variability and overlap, each disease has a typical regional pattern of hypometabolism caused by the typical regional pattern of neurodegeneration.[5] These patterns match those previously identified in studies using perfusional single photon emission tomography (SPECT) with ^{99m}Tc-ethyl cysteinate dimer (ECD) and ^{99m}Tc-hexamethylpropyleneamine oxime (HMPAO), which measure the patterns of regional hypoperfusion associated with neurodegeneration. Due to improved spatial resolution and better diagnostic accuracy,[6-8] ^{18}F-FDG PET has largely replaced perfusion

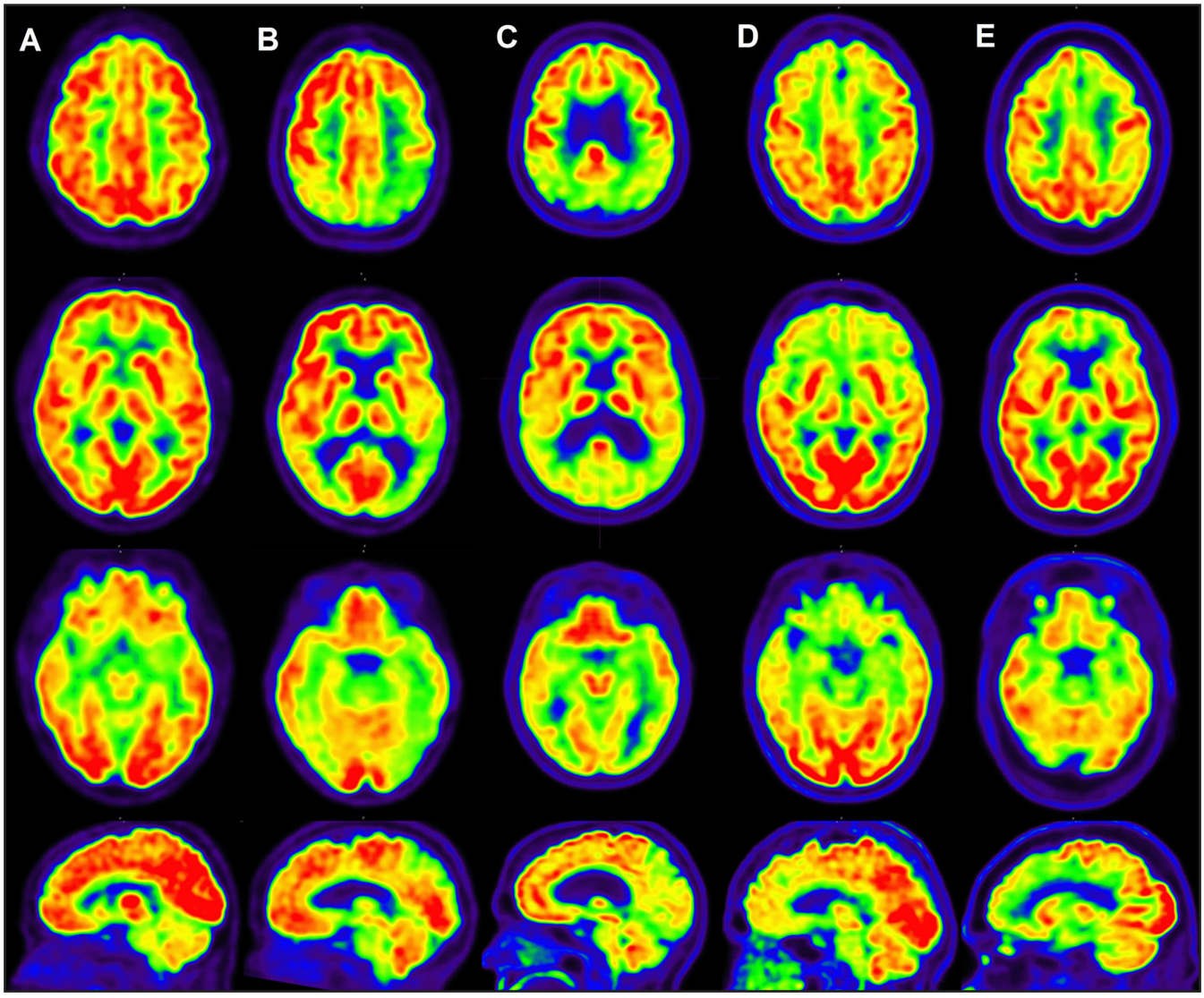

FIGURE 1. *Typical appearance of neurodegenerative dementias on ^{18}F-FDG PET. (A) Normal ^{18}F-FDG PET brain PET. (B) Typical AD pattern with decreased metabolic activity in the posterior cingulate gyrus and temporal and parietal lobes. (C) Classic DLB with decreased metabolic activity in occipital lobe and preserved posterior cingulate uptake. (D) Typical behavioral variant of FTLD with decreased metabolic activity in frontal lobes and anterior temporal lobes. (E) Semantic variant of FTLD with asymmetrically decreased metabolic activity involving the left perisylvian region. The top row of images is through the superior frontal and parietal lobes; the second row through the basal ganglia; the third row through the temporal and occipital lobes; and the fourth row shows a parasagittal slice.*

SPECT in evaluating cognitive decline and dementia in clinical practice. As a topographic marker of neurodegeneration, the hypometabolism pattern on ^{18}F-FDG PET is affected by individual variability in neurodegeneration pattern.[9,10] This variability is best seen in several atypical but well characterized presentations of neurodegenerative diseases that may show patterns that differ from the archetype.

Under the current Centers for Medicare & Medicaid Services (CMS) coverage guidelines, ^{18}F-FDG is approved clinically for differential diagnosis of AD versus FTLD in patients with cognitive decline of at least six months' duration and who meet diagnostic criteria for both.[11-13] The use of ^{18}F-FDG for this indication is based upon strong evidence that typical presentations of these diseases show clearly different patterns of hypometabolism.[5,9,14] However, multiple studies have also shown efficacy in differential diagnosis of other neurodegenerative diseases.[5,9,14]

Typical patterns of ^{18}F-FDG PET in neurodegenerative diseases

Classically in AD, ^{18}F-FDG PET shows most prominently decreased metabolic activity in the lateral temporoparietal cortices, precuneus, posterior cingulate cortices, and medial temporal lobes, including the hippocampi. The posterior cingulate cortex is one of the most specific regions of abnormality in AD on ^{18}F-FDG PET,[8,10] and it must be specifically evaluated in each case. The frontal lobes are also frequently

involved later in the disease course, usually to a lesser degree than the temporal/parietal lobes (**Figure 1A/B**). These changes are typically bilateral and symmetric, but they can show some asymmetry. When this pattern of hypometabolism, albeit usually less severe, is seen in MCI patients, it suggests underlying AD pathology and future progression to AD. In typical AD, metabolism in the occipital and somatosensory cortex, as well as the deep cerebral nuclei, is preserved.[8,9]

In DLB, where cognitive decline may be accompanied with hallucinations, sleep disorder, and parkinsonism, decreased metabolic activity in the occipital lobes may allow discrimination from AD. Otherwise, DLB also shows hypometabolism in many regions involved in AD, including the temporoparietal and frontal cortex (**Figure 1C**). Also suggestive of the diagnosis of DLB is preservation of posterior cingulate cortex uptake with hypometabolism in the adjacent precuneus and cuneus, termed the "cingulate island sign".[15-17] In cases of DLB without AD pathology, there is also sparing of medial temporal metabolism. However, in about 70% of cases of DLB, there is coexistent AD pathology,[18] likely accounting for a part of the overlap in metabolic pattern between DLB and AD.

FTLD consists of a group of clinically and pathologically heterogeneous neurodegenerative conditions with varied clinical features but overlapping underlying pathologic and genetic etiologies; as a result, FTLD can show one of several patterns on ^{18}F-FDG PET. In the behavioral variant of FTLD, characterized by personality and emotional changes and originally called Pick's disease, cerebral hypometabolism is seen in the frontal lobes, commonly with involvement of the anterior cingulate cortex and variable involvement of the anterior temporal lobes (**Figure 1D**).[8,9,19] In the semantic dementia variant of FTLD, associated with loss of ability to understand word meaning, there is asymmetric left-predominant anterior temporal lobe hypometabolism (**Figure 1E**).[9,20] The progressive nonfluent aphasia variant of FTLD, clinically associated with inability to produce language, is characterized by asymmetric left anterior perisylvian hypometabolism. Rarely, FTLD can show a pattern of hypometabolism similar to classic AD, although frontal hypometabolism is usually also seen in these cases.[19,21-23]

Overall, although ^{18}F-FDG is not a biomarker specific to a single dementia entity, there is a strong body of evidence on its high sensitivity and specificity in differentiating dementia types.[9,10,14] Perhaps as important, a normal ^{18}F-FDG PET scan dramatically reduces the probability of an underlying neurodegenerative cause of a patient's clinical symptoms and portends a favorable prognosis.

Atypical patterns on ^{18}F-FDG PET

Several factors affect the sensitivity and specificity of ^{18}F-FDG PET in neurodegenerative dementia. These include variants of AD with unusual patterns of neurodegeneration, non-neurodegenerative diseases, of which vascular dementia is the most common, and the effects of medications.[24-27]

Several atypical, non-amnestic presentations of AD comprise about one-third of young-onset AD cases and about 5% of late-onset AD cases.[28] These presentations exhibit different patterns of cerebral hypometabolism with regional involvement that matches the specific patterns of cognitive decline.[23,29] The logopenic variant of primary progressive aphasia is usually due to AD but with primary impairment in language, specifically word repetition, and shows asymmetric left temporoparietal hypometabolism.[23] This pattern can be similar to one of the language variants of FTLD. The posterior cortical atrophy variant of AD, with a characteristic visuospatial impairment, tends to have symmetric parietal-occipital hypometabolism, a pattern overlapping with DLB.[30]

Hypometabolism in the deep gray nuclei is atypical for AD, FTLD, and DLB in the absence of severe cortical atrophy. Involvement of these structures should raise consideration of other etiologies, ranging from vascular dementia to rare neurodegenerative conditions such as corticobasal degeneration or secondary neurodegenerative diseases like Creutzfeld-Jacob disease. Vascular dementia is relatively common, accounting for 10-20% of dementia.[31,32] It is caused by microvascular ischemia and/or multiple infarctions and is highly linked with cardiovascular risk factors. Vascular dementia can result in atypical patterns of hypometabolism on ^{18}F-FDG PET commonly affecting the deep gray structures and frontal lobes, but with variability depending on the vascular territories affected in an individual case.[33] As vascular abnormality is frequently seen along with AD, this may account for some atypical metabolic patterns in AD patients.

Centrally active medications can have effects on cerebral metabolism, particularly during periods of medication changes as the brain adjusts to the new equilibrium. Barbiturates and sedatives have the strongest effects; however, other medications, including narcotics, antipsychotics, and corticosteroids, can have an effect.[34,35] Medication-induced hypometabolism can mask an underlying neurodegenerative condition.

Amyloid PET in neurodegeneration

Two hallmark pathologic protein aggregates are present in the brain of AD patients: ß-amyloid neuritic plaques and tau-containing neurofibrillary tangles. The development of ^{11}C Pittsburgh Compound B (^{11}C-PiB) PET just over one decade ago allowed in vivo imaging of ß-amyloid plaques.[36,37] Due to the short, 20.3-minute half-life of the ^{11}C radioisotope, it is not possible to produce ^{11}C-PiB for widespread use. Subsequently, three fluorinated amyloid PET tracers (^{18}F-florbetaben, ^{18}F-florbetapir, and ^{18}F-flutemetamol) were developed and approved by the U.S. Food and Drug Administration (FDA)

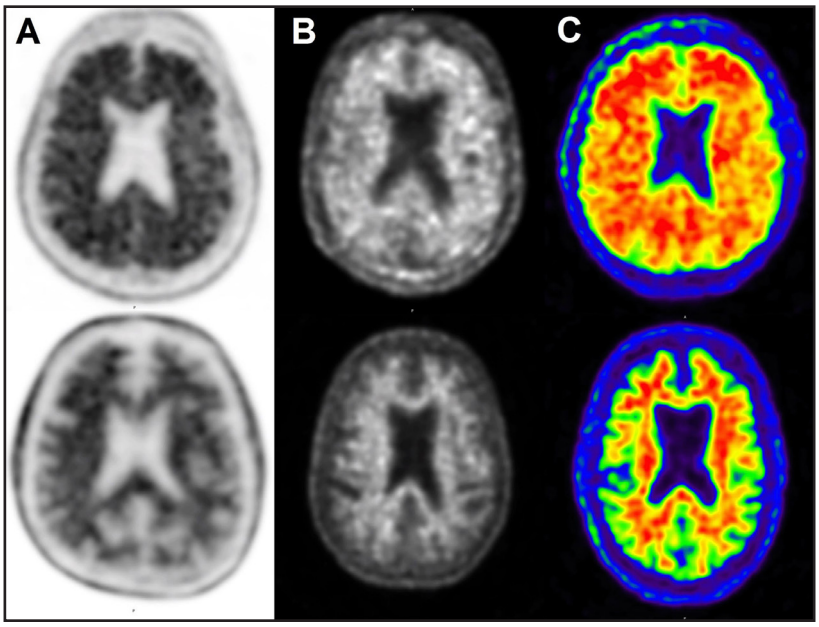

FIGURE 2. *Positive and negative amyloid PET scans using ^{18}F-florbetapir (A), ^{18}F-florbetaben (B), and ^{18}F-flutemetamol (C). The presence of cortical binding for all three radiotracers indicates the presence of moderate to severe amyloid plaque. Note the presence of prominent white matter tracer uptake in these commercially available ^{18}F amyloid PET tracers.*

for clinical use. [38-40] Due to more prominent, nonspecific white matter tracer binding, as part of the FDA approval process, all commercial vendors have been required to develop reader-training programs to ensure that readers appropriately detect the pathological cortical radiotracer binding. Imagers must complete this training and follow the specific guidelines described for each radiotracer in order to interpret amyloid PET studies. Clinically, amyloid PET is interpreted as either positive or negative for the presence of cortical ß-amyloid plaque (**Figure 2**). High inter-reader agreement can be achieved for amyloid PET.[41]

The three FDA-approved amyloid PET radiotracers have high sensitivity for beta-amyloid deposition, with intensity of binding correlated with burden of amyloid plaque on histopathology.[42-46] Specificity for amyloid plaque is also high. Patients with AD are nearly uniformly positive on amyloid PET. In addition, studies have shown that detectable cortical amyloid is present in approximately 50% of MCI patients,[47] and that these amyloid-positive MCI patients are more likely to progress to AD.[44,48,49] However, the detection of cerebral cortical amyloid deposition does not indicate that an individual has or will develop AD. Deposition of cortical amyloid plaque is commonly seen with aging, even in people without cognitive symptoms, with 10-15% at age 60 years old to approximately 50% at 80 years showing detectable cortical amyloid.[50] As a result, the specificity and positive predictive value of amyloid PET for AD declines with increasing age.[47,51]

On the other hand, a negative amyloid PET scan indicates that there is no significant cerebral ß-amyloid plaque, which is incompatible with a diagnosis of AD and should direct clinicians to search for alternative etiologies. To help narrow the use of amyloid PET to a population that is most likely to benefit, the Alzheimer's Association and Society for Nuclear Medicine and Molecular Imaging published a set of appropriateness criteria, summarized in the Table.[52] Note that a growing body of evidence shows that cerebral amyloid may start accumulating decades before onset of dementia and may even have detrimental effects even in cognitively normal patients;[47,51] however, due to a lack of efficacious preventive therapies, these groups are not likely to benefit from knowledge of amyloid status.

The various subtypes of FTLD are associated with several different pathologic protein aggregates, most commonly containing either tau protein or TDP-43 (transactive response DNA binding protein, 43 kDa).[53] Due to the absence of amyloid pathology and typically younger age of presentation of FTLD, studies have shown high negative amyloid PET rates in FTLD as well as strong ability to distinguish AD from FTLD.[54-56] Positive amyloid scans in FTLD groups may represent clinical misdiagnosis or presence of multiple pathologies.

In contrast, about 70% of DLB patients have cerebral amyloid deposition,[18] most of which meet pathologic criteria for mixed DLB-AD.[47,57] Although cognitive features are initially most prominent, DLB patients ultimately develop parkinsonism. Clinically, DLB is distinguished from Parkinson disease (PD) with dementia by dementia preceding or manifesting within one year after the onset of a Parkinsonian movement disorder.[58] Like Parkinson disease, the hallmark protein aggregates in DLB are α-synuclein-containing Lewy bodies, for which there is currently no clinically available radiotracer. However, as with PD, DLB shows decreased striatal uptake on molecular imaging of the dopaminergic system,[59,60] with ^{123}I-ioflupane SPECT being the most widely used tracer in the US.

Recent developments

Historically, medical images have been interpreted visually, with quantification largely restricted to the research arena. As demonstrated with measurements of hippocampal volume and cortical thickness decreases in AD on structural MRI, quantification can provide information that is difficult or impossible to see with the human eye with high accuracy and precision. Furthermore, quantification can reliably

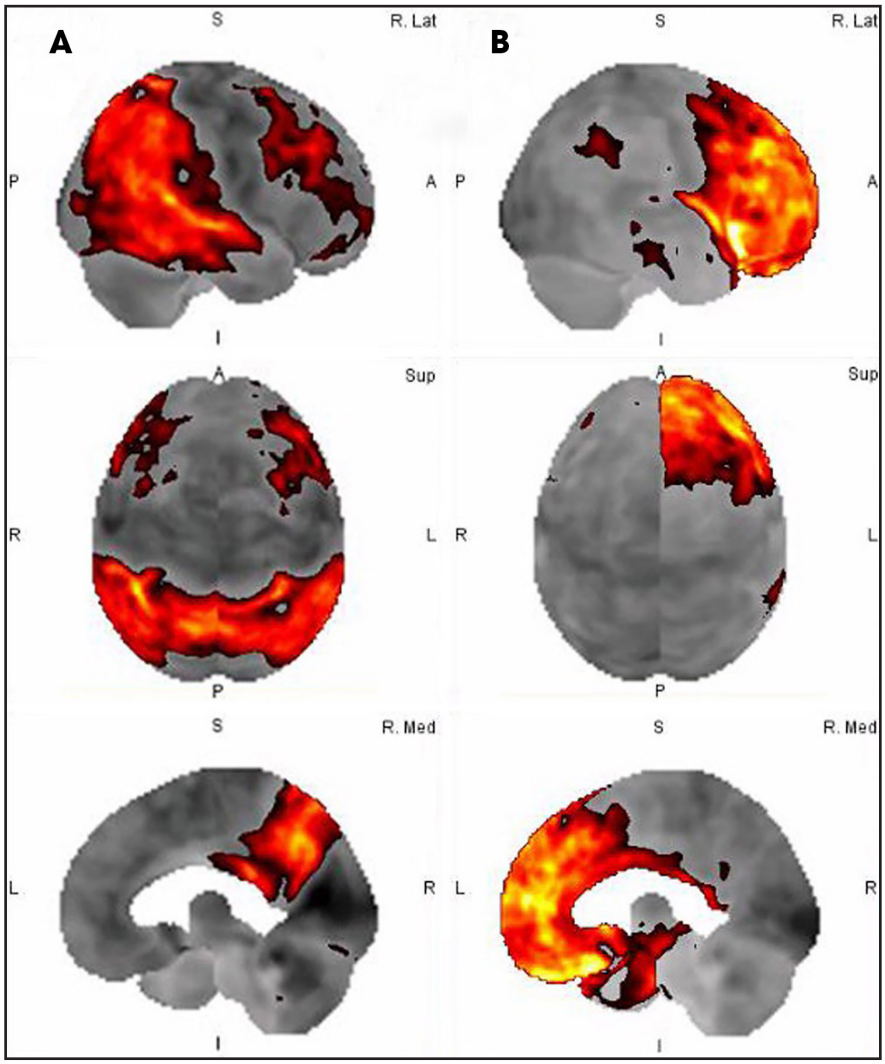

FIGURE 3. *Voxel-based analysis of ^{18}F-FDG PET brain scans of two patients, with regions of decreased metabolic activity compared to normal database highlighted in color. (A) AD patient with decreased metabolic activity in the posterior cingulate gyrus and temporal and parietal lobes, as well as milder involvement of the frontal lobes. (B) FTLD patient with asymmetric decreased metabolic activity predominantly in the left frontal lobe, left anterior temporal lobes, and left anterior cingulate gyrus. Analysis was performed using MIMneuro (Version 6.4.9, MIM Software, Inc., Cleveland, OH).*

demonstrate subtle changes over time that carry important diagnostic and prognostic information. PET is intrinsically quantifiable, as intensity directly reflects radioligand binding. ^{18}F-FDG binding is correlated with cerebral metabolism and amyloid PET radiotracers correlate with cerebral amyloid burden.[42,61] Techniques for quantification are starting to gain acceptance in clinical image interpretation.

For brain ^{18}F-FDG PET, many commercial software packages are available to compare a patient's scan to a database of controls, often matched for age and gender. These analyses are most often performed on a voxel-by-voxel basis to quantify metabolic changes across the whole brain. For example, **Figure 3** depicts the results from voxel-based analysis for an AD patient (**Figure 3A**) and a FTLD patient (**Figure 3B**), with areas of decreased metabolic activity compared to the normal database highlighted in color. These analytic software packages aid the imaging specialist in visualizing the overall pattern of decreased cerebral metabolic activity. The required complex computational steps of co-registration and voxel-based comparisons can generate errors, particularly if there is asymmetric/focal atrophy, so correlation with direct evaluation of the patient's images remains critical.

Although unassisted visual interpretation of amyloid PET is mandated by the reader training programs, there are several factors to suggest that value of amyloid PET will be improved with quantification. First, studies have shown that quantification improves reader agreement.[41,43] Amyloid PET, while sensitive, shows a low increase in signal between negative and positive[42] and high non-target white matter binding that can make detection of cortical binding challenging for the human eye, particularly in borderline cases. Amyloid PET is typically quantified as a standardized uptake value ratio,[62] where individual voxel uptake is normalized to a reference region. Historically, cerebellar uptake has been used as reference, as the cerebellum is known to have little amyloid deposition even in advanced AD, although recent studies suggest that whole white matter uptake may be more reliable, especially in longitudinal follow up.[63,64] This simple SUVR quantification method allows comparison between individuals and to normal values, and evaluation of change over time.[65] The precise role of quantification for clinical amyloid PET requires further investigation.

Future directions

The advancements in ^{18}F-FDG PET and amyloid PET have contributed tremendously toward understanding the underlying pathophysiology of neurodegenerative dementia, and the future continues to look promising. While both ^{18}F-FDG PET and amyloid PET have demonstrated robust clinical performance,[66] their role in the clinic in the setting of other imaging and laboratory biomarkers that have been developed as AD continues to evolve. The *Imaging Dementia – Evidence for Amyloid Scanning (IDEAS)*

Table. Summary of Appropriate Use Criteria for Amyloid PET (Adapted from Johnson, et al., 2013)[48]

Current evidence supports the use of amyloid PET in patients who meet all these criteria:

1. Objectively confirmed cognitive impairment
2. Uncertain diagnosis after comprehensive evaluation by a dementia expert, with AD as a possible diagnosis
3. Result of amyloid PET expected to increase diagnostic certainty and alter management
4. Patient has persistent or unexplained MCI

or

Patient meets core clinical criteria for possible AD71 due to either atypical clinical course or mixed presentation

or

Patient has atypical early onset of progressive dementia before 65 years of age

Examples of inappropriate use scenarios

1. Patients with high certainly for AD diagnosis, meeting clinical criteria for probable AD with typical age of onset
2. Patients without objective cognitive decline, regardless of subjective deficits, positive family history, or known genetic mutation)
3. Non-medical use

Study, which aims to evaluate the clinical effect of amyloid PET on patient management and outcomes, has been enrolling subjects since early 2016, provides temporary Medicare reimbursement for clinical amyloid PET scans that meet appropriate use criteria for the first time (**Table**). Ultimately, the clinical fate of amyloid PET most likely depends on future development of disease-modifying therapies.

Beyond these established radiotracers, novel tracers in various stages of development aim to target other critical protein aggregates in neurodegeneration such as tau[67,68] and alpha-synuclein.[69] In the near future, it may be possible to evaluate and quantify the presence of several pathologic protein aggregates to facilitate improved and earlier diagnosis and hopefully provide improved estimation of a patient's future clinical course.

REFERENCES

1. 2012 Alzheimer's disease facts and figures. *Alzheimers Dement.* 2012;8(2):131-68.
2. Brookmeyer R, Johnson E, Ziegler-Graham K, Arrighi HM. Forecasting the global burden of Alzheimer's disease. *Alzheimers Dement.* 2007;3(3):186-91.
3. van der Flier WM, Scheltens P. Epidemiology and risk factors of dementia. *J Neurol Neurosurg Psychiatry.* 2005;76 Suppl 5:v2-7.
4. Nasrallah I, Dubroff J. An overview of PET neuroimaging. *Semin Nucl Med.* 2013;43(6):449-61.
5. Teune LK, Bartels AL, de Jong BM, et al. Typical cerebral metabolic patterns in neurodegenerative brain diseases. *Mov Disord.* 2010;25(14): 2395-2404.
6. Herholz K, Schopphoff H, Schmidt M, et al. Direct comparison of spatially normalized PET and SPECT scans in Alzheimer's disease. *J Nucl Med.* 2002;43(1):21-6.
7. Rahmim A, Zaidi H. PET versus SPECT: strengths, limitations and challenges. *Nucl Med Commun.* 2008;29(3):193-207.
8. Silverman DH. Brain 18F-FDG PET in the diagnosis of neurodegenerative dementias: comparison with perfusion SPECT and with clinical evaluations lacking nuclear imaging. *J Nucl Med.* 2004;45(4):594-607.
9. Brown RK, Bohnen NI, Wong KK, Minoshima S, Frey KA. Brain PET in suspected dementia: patterns of altered FDG metabolism. *Radiographics.* 2014;34(3):684-701.
10. Nasrallah IM, Wolk DA. Multimodality imaging of Alzheimer disease and other neurodegenerative dementias. *J Nucl Med.* 2014;55(12):2003-11.
11. National Coverage Determination (NCD) for FDG PET for Dementia and Neurodegenerative Diseases (220.6.13). 2009; https://www.cms.gov/medicare-coverage-database/details/ncd-details.aspx?NCDId=288&ncdver=3&bc=BAABAAAAAAAA&. Accessed December 23, 2015.
12. Foster NL, Heidebrink JL, Clark CM, et al. FDG-PET improves accuracy in distinguishing frontotemporal dementia and Alzheimer's disease. *Brain.* 2007;130(Pt 10):2616-35.
13. Ibach B, Poljansky S, Marienhagen J, Sommer M, Manner P, Hajak G. Contrasting metabolic impairment in frontotemporal degeneration and early onset Alzheimer's disease. *Neuroimage.* 2004;23(2):739-43.
14. Bohnen NI, Djang DS, Herholz K, Anzai Y, Minoshima S. Effectiveness and safety of 18F-FDG PET in the evaluation of dementia: a review of the recent literature. *J Nucl Med.* 2012;53(1): 59-71.
15. Graff-Radford J, Murray ME, Lowe VJ, et al. Dementia with Lewy bodies: basis of cingulate island sign. *Neurology.* 2014;83(9):801-9.
16. Imamura T, Ishii K, Sasaki M, et al. Regional cerebral glucose metabolism in dementia with Lewy bodies and Alzheimer's disease: a comparative study using positron emission tomography. *Neurosci Lett.* 1997;235(1-2):49-52.
17. Lim SM, Katsifis A, Villemagne VL, et al. The 18F-FDG PET cingulate island sign and comparison to 123I-beta-CIT SPECT for diagnosis of dementia with Lewy bodies. *J Nucl Med.* 2009;50(10):1638-45.
18. Weisman D, McKeith I. Dementia with Lewy bodies. *Seminars in neurology.* 2007;27(1):42-7.
19. Diehl-Schmid J, Grimmer T, Drzezga A, et al. Decline of cerebral glucose metabolism in frontotemporal dementia: a longitudinal 18F-FDG-PET-study. *Neurobiol Aging.* 2007;28(1):42-50.
20. Diehl-Schmid J, Grimmer T, Drzezga A, et al. Longitudinal changes of cerebral glucose metabolism in semantic dementia. *Dement Geriatr Cogn Disord.* 2006;22(4):346-51.
21. Jacova C, Hsiung GY, Tawankanjanachot I, et al. Anterior brain glucose hypometabolism predates dementia in progranulin mutation carriers. *Neurology.* 2013;81(15):1322-31.
22. Perani D, Della Rosa PA, Cerami C, et al. Validation of an optimized SPM procedure for FDG-PET in dementia diagnosis in a clinical setting. *Neuroimage Clin.* 2014;6:445-54.
23. Rabinovici GD, Jagust WJ, Furst AJ, et al. Abeta amyloid and glucose metabolism in three variants of primary progressive aphasia. *Ann Neurol.* 2008;64(4):388-401.
24. Berti V, Mosconi L, Pupi A. Brain: normal variations and benign findings in fluorodeoxyglucose-PET/computed tomography imaging. *PET Clin.* 2014;9(2):129-40.
25. Mielke R, Heiss WD. Positron emission tomography for diagnosis of Alzheimer's disease and vascular dementia. *J Neural Transm Suppl.* 1998;53:237-50.
26. Bergeron D, Beauregard JM, Guimond J, et al. Clinical Impact of a Second FDG-PET in Atypical/Unclear Dementia Syndromes. *J Alzheimers Dis.* 2015;49(3):695-705.
27. Madhavan A, Whitwell JL, Weigand SD, et al. FDG PET and MRI in logopenic primary progressive aphasia versus dementia of the Alzheimer's type. *PLoS One.* 2013;8(4):e62471.
28. Koedam EL, Lauffer V, van der Vlies AE, van der Flier WM, Scheltens P, Pijnenburg YA. Early-versus late-onset Alzheimer's disease: more than age alone. *J Alzheimers Dis.* 2010;19(4):1401-8.

29. Gorno-Tempini ML, Dronkers NF, Rankin KP, et al. Cognition and anatomy in three variants of primary progressive aphasia. *Ann Neurol.* 2004;55(3):335-46.
30. Laforce R, Jr., Tosun D, Ghosh P, et al. Parallel ICA of FDG-PET and PiB-PET in three conditions with underlying Alzheimer's pathology. *Neuroimage Clin.* 2014;4:508-16.
31. Fratiglioni L, Launer LJ, Andersen K, et al. Incidence of dementia and major subtypes in Europe: A collaborative study of population-based cohorts. Neurologic Diseases in the Elderly Research Group. *Neurology.* 2000;54(11 Suppl 5):S10-5.
32. Lobo A, Launer LJ, Fratiglioni L, et al. Prevalence of dementia and major subtypes in Europe: A collaborative study of population-based cohorts. Neurologic Diseases in the Elderly Research Group. *Neurology.* 2000;54(11 Suppl 5):S4-9.
33. Pascual B, Prieto E, Arbizu J, Marti-Climent J, Olier J, Masdeu JC. Brain glucose metabolism in vascular white matter disease with dementia: differentiation from Alzheimer disease. *Stroke.* 2010;41(12):2889-93.
34. Brunetti A, Fulham MJ, Aloj L, et al. Decreased brain glucose utilization in patients with Cushing's disease. *J Nucl Med.* 1998;39(5):786-90.
35. Theodore WH. Antiepileptic drugs and cerebral glucose metabolism. *Epilepsia.* 1988;29 Suppl 2:S48-55.
36. Klunk WE, Engler H, Nordberg A, et al. Imaging brain amyloid in Alzheimer's disease with Pittsburgh Compound-B. *Ann Neurol.* 2004;55(3):306-19.
37. Klunk WE, Wang Y, Huang GF, et al. The binding of 2-(4'-methylaminophenyl)benzothiazole to postmortem brain homogenates is dominated by the amyloid component. *J Neurosci.* 2003;23(6):2086-92.
38. FDA approves 18F-florbetapir PET agent. *J Nucl Med.* 2012;53(6):15N.
39. GE beta-amyloid agent approved. *J Nucl Med.* 2013;54(12):10N.
40. Jeffrey S. FDA Approves Third Amyloid PET Tracer for Alzheimer's. 2014; http://www.medscape.com/viewarticle/822370. Accessed December 27, 2015.
41. Nayate AP, Dubroff JG, Schmitt JE, et al. Use of Standardized Uptake Value Ratios Decreases Interreader Variability of [18F] Florbetapir PET Brain Scan Interpretation. *AJNR Am J Neuroradiol.* 2015;36(7):1237-44.
42. Clark CM, Schneider JA, Bedell BJ, et al. Use of florbetapir-PET for imaging beta-amyloid pathology. *Jama.* 2011;305(3):275-83.
43. Mountz JM, Laymon CM, Cohen AD, et al. Comparison of qualitative and quantitative imaging characteristics of [(11)C]PiB and [(18)F] flutemetamol in normal control and Alzheimer's subjects. *Neuroimage Clin.* 2015;9:592-8.
44. Schreiber S, Landau SM, Fero A, Schreiber F, Jagust WJ. Comparison of Visual and Quantitative Florbetapir F 18 Positron Emission Tomography Analysis in Predicting Mild CognitiveImpairmentOutcomes.*JAMANeurol.*2015;72(10):1183-1190.
45. Tiepolt S, Barthel H, Butzke D, et al. Influence of scan duration on the accuracy of beta-amyloid PET with florbetaben in patients with Alzheimer's disease and healthy volunteers. *Eur J Nucl Med Mol Imaging.* 2013;40(2):238-44.
46. Wolk DA, Grachev ID, Buckley C, et al. Association between in vivo fluorine 18-labeled flutemetamol amyloid positron emission tomography imaging and in vivo cerebral cortical histopathology. *Arch Neurol.* 2011;68(11):1398-403.
47. Ossenkoppele R, Jansen WJ, Rabinovici GD, et al. Prevalence of amyloid PET positivity in dementia syndromes: a meta-analysis. *Jama.* 2015;313(19):1939-49.
48. Doraiswamy PM, Sperling RA, Coleman RE, et al. Amyloid-beta assessed by florbetapir F 18 PET and 18-month cognitive decline: a multicenter study. *Neurology.* 2012;79(16):1636-44.
49. Doraiswamy PM, Sperling RA, Johnson K, et al. Florbetapir F 18 amyloid PET and 36-month cognitive decline:a prospective multicenter study. *Mol Psychiatry.* 2014.
50. Rowe CC, Ellis KA, Rimajova M, et al. Amyloid imaging results from the Australian Imaging, Biomarkers and Lifestyle (AIBL) study of aging. *Neurobiol Aging.* 2010;31(8):1275-83.
51. Jansen WJ, Ossenkoppele R, Knol DL, et al. Prevalence of cerebral amyloid pathology in persons without dementia: a meta-analysis. *Jama.* 2015;313(19):1924-38.
52. Johnson KA, Minoshima S, Bohnen NI, et al. Appropriate use criteria for amyloid PET: a report of the Amyloid Imaging Task Force, the Society of Nuclear Medicine and Molecular Imaging, and the Alzheimer's Association. *J Nucl Med.* 2013;54(3):476-90.
53. Neumann M, Sampathu DM, Kwong LK, et al. Ubiquitinated TDP-43 in frontotemporal lobar degeneration and amyotrophic lateral sclerosis. *Science.* 2006;314(5796):130-3.
54. Kobylecki C, Langheinrich T, Hinz R, et al. 18F-florbetapir PET in patients with frontotemporal dementia and Alzheimer disease. *J Nucl Med.* 2015;56(3):386-91.
55. Rabinovici GD, Rosen HJ, Alkalay A, et al. Amyloid vs FDG-PET in the differential diagnosis of AD and FTLD. *Neurology.* 2011;77(23):2034-42.
56. Rabinovici GD, Furst AJ, O'Neil JP, et al. 11C-PIB PET imaging in Alzheimer disease and frontotemporal lobar degeneration. *Neurology.* 2007;68(15):1205-12.
57. Villemagne VL, Ong K, Mulligan RS, et al. Amyloid imaging with (18)F-florbetaben in Alzheimer disease and other dementias. *J Nucl Med.* 2011;52(8):1210-7.
58. Chung EJ, Babulal GM, Monsell SE, Cairns NJ, Roe CM, Morris JC. Clinical Features of Alzheimer Disease With and Without Lewy Bodies. *JAMA Neurol.* 2015;72(7):789-96.
59. McKeith I, O'Brien J, Walker Z, et al. Sensitivity and specificity of dopamine transporter imaging with 123I-FP-CIT SPECT in dementia with Lewy bodies: a phase III, multicentre study. *Lancet Neurol.* 2007;6(4):305-13.
60. O'Brien JT, Colloby S, Fenwick J, et al. Dopamine transporter loss visualized with FP-CIT SPECT in the differential diagnosis of dementia with Lewy bodies. *Arch Neurol.* 2004;61(6):919-925.
61. Yamaji S, Ishii K, Sasaki M, et al. Evaluation of standardized uptake value to assess cerebral glucose metabolism. *Clin Nucl Med.* 2000;25(1):11-6.
62. Wong DF, Rosenberg PB, Zhou Y, et al. In vivo imaging of amyloid deposition in Alzheimer disease using the radioligand 18F-AV-45 (florbetapir [corrected] F 18). *J Nucl Med.* 2010;51(6):913-20.
63. Brendel M, Hogenauer M, Delker A, et al. Improved longitudinal [(18)F]-AV45 amyloid PET by white matter reference and VOI-based partial volume effect correction. *Neuroimage.* 2015;108:450-9.
64. Chen K, Roontiva A, Thiyyagura P, et al. Improved power for characterizing longitudinal amyloid-beta PET changes and evaluating amyloid-modifying treatments with a cerebral white matter reference region. *J Nucl Med.* 2015;56(4):560-6.
65. Saint-Aubert L, Nemmi F, Peran P, et al. Comparison between PET template-based method and MRI-based method for cortical quantification of florbetapir (AV-45) uptake in vivo. *Eur J Nucl Med Mol Imaging.* 2014;41(5):836-43.
66. Sanchez-Juan P, Ghosh PM, Hagen J, et al. Practical utility of amyloid and FDG-PET in an academic dementia center. *Neurology.* 2014;82(3):230-8.
67. Okamura N, Furumoto S, Harada R, et al. Novel 18F-labeled arylquinoline derivatives for noninvasive imaging of tau pathology in Alzheimer disease. *J Nucl Med.* 2013;54(8):1420-7.
68. Chien DT, Bahri S, Szardenings AK, et al. Early clinical PET imaging results with the novel PHF-tau radioligand [F-18]-T807. *J Alzheimers Dis.* 2013;34(2):457-68.
69. Chu W, Zhou D, Gaba V, et al. Design, Synthesis, and Characterization of 3-(Benzylidene) indolin-2-one Derivatives as Ligands for alpha-Synuclein Fibrils. *J Med Chem.* 2015;58(15):6002-6017.